Tri Dasa Mega Vol. 27 No. 2 (2005) 105–115

Jurnal Teknologi Reaktor Nuklir

Tri Dasa Mega

Journal homepage: https://ejurnal.brin.go.id/tridam

Boron Neutron Capture Therapy (BNCT) Dose Optimization for Esophageal Cancer Using Particle and Heavy Ion Transport Code System (PHITS) Ver. 3.35

Putri Nur Cahyani[1*], Mokhamad Tirono[1], Yohannes Sardjono[2], Isman Mulyadi Triatmoko[2], Gede Sutrisna[2], Fendinugroho[2], Nunung Nuraeni[2], Heru Prasetio[2]

[1]Department of Physics, Faculty of Science and Technology, Maulana Malik Ibrahim State Islamic University of Malang, Indonesia
[2]Research Center for Safety, Meteorology and Nuclear Quality Technology, Research Organization for Nuclear Energy, National Research and Innovation Agency, Indonesia.

ARTICLE INFO

Article history:

Received: August 22, 2025
Received in revised form: Oct. 10, 2025
Accepted: November 26, 2025

Keywords:

BNCT
PHITS
Dosimetry
Esophageal Cancer
Radiation Direction

A B S T R A C T

Esophageal cancer is a type of cancer that has a globally high incidence and mortality rate. Boron Neutron Capture Therapy (BNCT) is a promising radiation therapy method in esophageal cancer treatment due to its ability to deliver high doses selectively to tumor tissue with minimal impact on surrounding healthy tissue. This study aims to optimize BNCT dose distribution, evaluate the irradiation time, and determine the most effective irradiation direction in esophageal cancer. Simulations in this study were carried out using PHITS version 3.35 to model the geometry of esophageal cancer, surrounding organs, and radiation sources used. The phantom represented an ORNL adult male with a 24,69 cm^2 tumor. The neutron source came from an accelerator with a 30 MeV proton beam. The boron concentrations analyzed in the cancer tissue were 110, 125, and 140 μg/g. Irradiation from the posterior (PA) direction with a boron concentration of 140 μg/g showed the most optimal BNCT therapy results, with an irradiation time of 15.78 minutes. This technique is capable of delivering an effective dose to the cancerous tissue without exceeding the tolerance limits of the surrounding healthy organs, making it safe for use.

1. INTRODUCTION

Cancer is a major health concern, with 20 million new cases worldwide also causing 9.7 million deaths in 2020 [1]. A common type of cancer is esophageal cancer, ranking 11th worldwide in frequency and being the 7th leading cause of cancer death. Globally, there are an estimated 511.054 new cases of esophageal cancer and 445.391 deaths in 2022 [2]. Two of the main factors causing esophageal cancer are alcohol and smoking [3]. The prevalence of daily smoking among men in Indonesia is 54.4%, contributing to high cases of lung cancer and esophageal cancer [1].

Esophageal cancer is most commonly found in the mid-thoracic esophagus, and squamous cell carcinoma is the predominant histologic type [4]. The early stages of esophageal cancer appear as

* Corresponding author. Tel./Fax.: ……
Email:puputnc160@gmail.com
DOI:10.55981.tdm.2025.13333

polypoid growths or plaques [5]. Imaging methods are an important diagnostic step in identifying and staging esophageal cancer [6]. Some of the imaging techniques used in diagnosing and staging esophageal cancer include endoscopic ultrasonography, CT-scan, PET-CT, and MRI [7]. These imaging results form the basis for esophageal cancer treatment, such as radiation therapy [8]. BNCT is a next-generation radiotherapy that can kill cancer cells better than other radiation therapies, such as X-ray radiation and Proton Beam Therapy[9]. An illustration of the BNCT reaction and mechanism of action can be seen in Figure 1.

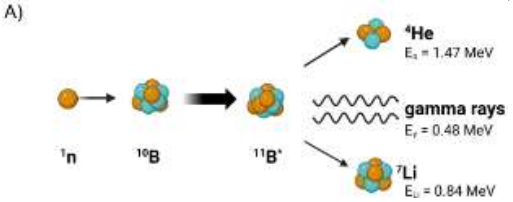

Figure 1. Reaction between thermal neutrons and B-10 in BNCT, producing alpha particles and lithium.

BNCT achieves selective therapy of cancer cells, and its effectiveness largely depends on the selective accumulation of ^{10}B in cancer cells with concurrent boron preparation[10]. BNCT utilizes the nuclear reaction of $^{10}B(n,\alpha)^{7}Li$ when stable ^{10}B interacts with thermal neutrons [11] to yield linear energy transfer of alpha particles (^{4}He) and recoiling lithium-7 (^{7}Li) [12]. Particles with high LET will preferentially damage only tumor cells and preserve surrounding normal cells [13]. The success of BNCT is highly dependent on the selective accumulation of ^{10}B in cancer cells by the administered boron preparation and the neutron source [10]. The current neutron sources used in BNCT are Compact Accelerator-Based Neutron Sources, which are more effective than reactors [14].

To support and validate the application of BNCT in clinical and simulation settings, several previous studies have been conducted and serve as essential references for this research. Valeria Conte performed microdosimetry on boron for cancer with concentrations of 10-100 µg/g, with the most effective dose being 100 µg/g [11]. Xin Wang, MD, et.al. performed therapy on esophageal cancer using Proton Beam Therapy and Intensity Modulated Radiation Therapy [15]. Ryo Kakino proved that PHITS is validated for BNCT simulation and is able to model neutron and gamma distributions well [16].

There has been no previous study examining the dose and direction of radiation for BNCT in esophageal cancer, while the dose and direction of radiation are important in the BNCT implementation procedure. Therefore, this study was conducted. The radiation direction used was AP (Anterior-Posterior) to determine the most effective radiation direction in delivering the dose to cancer tissue and minimizing radiation exposure to healthy organs. The boron concentrations used were 110 µg/g, 125 µg/g, and 140 µg/g. These concentration levels were selected based on Valeria Conte's previous research. Her findings indicated that concentrations below 10 µg/g could result in minimal dose contribution and be less effective in targeting cancer cells. Meanwhile, a concentration of 100 µg/g is considered the most effective because it provides an optimal lethal dose to tumor tissue with a shorter exposure time and minimal risk to healthy tissue. The dose distribution and exposure time in BNCT were calculated using PHITS version 3.35 because of its advantages in speed and calculation accuracy.

2. THEORY

BNCT uses an accelerator-based neutron source to generate protons [17]. Protons are fired at targets such as beryllium or lithium and produce fast neutrons (>10 keV) [18]. Fast neutrons are moderated in the BSA into epithermal neutrons (0.5 eV-10 keV) and thermal neutrons (<0.5 eV) [14]. Thermal neutrons are suitable for treating low-depth cancers, and epithermal neutrons are suitable for treating deep cancers [19]. Neutrons only interact with cells that contain boron. Therefore, boron accumulation in cancer cells is very important to optimize BNCT [20].

Boron accumulation in BNCT depends on boron-carrying agents such as 4-Borono-L-Phenylalanine (BPA) and Sodium Mercapto undecahydro-closo-dodecaborate (BSH)[21]. BSH enters tumor cells through passive diffusion across the plasma membrane, which makes it evenly distributed. However, BSH does not cross the intact blood-brain barrier (BBB) [22]. BPA can be absorbed by various types of cancer cells due to the amino acid transport activity in the cells. BPA tends to stay longer in melanoma cells compared to other types of cancer cells [23]. Boron accumulated in cancer cells will react with neutrons from the accelerator source [24]. To calculate the accuracy of the reaction dose from the boron and neutrons in BNCT, simulations were carried out using the PHITS (Particle and Heavy Ion Transport code System) program [25].

PHITS is a general-purpose Monte Carlo method-based code for simulating radiation transport [26]. It is capable of modeling the movement of various types of particles, including ions with energies up to 1 TeV per nucleon [27].

PHITS can be used to calculate the average dose and 3D dose distribution, as well as provide more accurate dose estimation and a more precise projection of the dose absorbed by the patient [28]. PHITS is the most accurate component because it relies on the simulation of proton and ion transport via ATIMA (Atomic Interaction with Matter), and electron and positron transport using EGS5 (Electron Gamma Shower Version 5), which plays an important role [29].

BNCT has four dose components that are considered: gamma dose, boron dose, neutron dose, and proton dose. The dose rate values for these four components are obtained from the PHITS output and then processed using Microsoft Excel to calculate the equivalent dose rate, irradiation time, and equivalent dose. The total dose rate or equivalent dose rate is obtained from the sum of the dose rates from each source multiplied by the irradiation quality factor from the radiation source, as shown in Table 2. The total dose rate can be calculated using the formula in Eq. 1.

$$\mathrm{E}\left(\frac{Gy}{s}\right) = (CBE_B \times \dot{\mathrm{D}}_B) + (RBE_N \times \dot{\mathrm{D}}_N) + (RBE_H \times \dot{\mathrm{D}}_H) + (W_\gamma \times \dot{\mathrm{D}}_\gamma) \quad (1)$$

The $\dot{\mathrm{D}}_B$ is alpha dose, $\dot{\mathrm{D}}_N$ is neutron dose, $\dot{\mathrm{D}}_H$ is proton dose, and $\dot{\mathrm{D}}_\gamma$ is gamma dose [30]. The CBE and RBE values used are in Table 2 [31].

Table 1. CBE and RBE values

Tissue Type	CBE	RBE_N	RBE_H	RBEγ
Tumour	3.8	2.9	2.4	1
Skin	2.5	2.9	2.4	1
Bone	1	2.9	2.4	1
Soft Tissue	1.34	2.9	2.4	1

To kill cancer cells, BNCT requires an estimated therapy time. The irradiation time (t) needed to achieve the minimum dose value for the GTV can be determined. Irradiation time can be calculated using Eq. 2 [32].

$$\text{Irradiation time(s)} = \frac{minimum\ dose(Gy)}{Dtotal\ (Gy\,s)} \quad (2)$$

After the exposure time, the equivalent dose can be calculated from healthy and cancer tissue. The equivalent dose is used to determine the damage that occurs to healthy tissue around the tumor. The absorbed dose for each organ can be calculated using Eq. 3 [33].

$$D_{eq}\ \text{OAR (Gy)} = \left(\text{ED OAR } \left(\frac{Gy}{s}\right) \text{ x irradiation time (s)}\right) \quad (3)$$

3. METHODOLOGY

The instrumentation used to run a series of simulations in this research includes:

1. A portable computer with the following specifications: Snapdragon (TM) 860 @2.96 GHz (8 CPUs), 6 GB RAM, and a Windows 11 Pro 64-bit Operating System.
2. PHITS simulation program version 3.35.
3. Microsoft Word 2021.
4. Microsoft Excel 2021.
5. Notepad++.
6. Python
7. Google Collaboratory

3.1 Patient Model

The patient model uses geometric modeling based on the Oak Ridge National Laboratory (ORNL) adult male phantom model and body composition data from Report 145 of the International Commission on Radiological Protection (ICRP). The modeled cancer is a case of middle esophageal cancer depicted using CT-Scan in Figure 2 from Shanghai Cancer Center, Fudan University, Shanghai, China. The cancer was diagnosed as T3N1M0, indicating a cancer with Gross Tumor Volume (GTV) of 36.79 cm^3, Clinical Target Volume (CTV) of 139.53, and Primary Tumor Volume (PTV) with a margin of 0.5 cm from the CTV [34]. At risk of esophageal cancer are the heart, lungs, and stomach [35]. The results of the 2-dimensional geometric shape modeling of esophageal cancer can be seen in Figure 3.

Figure 2. Transverse CT-Scan images in patients with esophageal cancer.

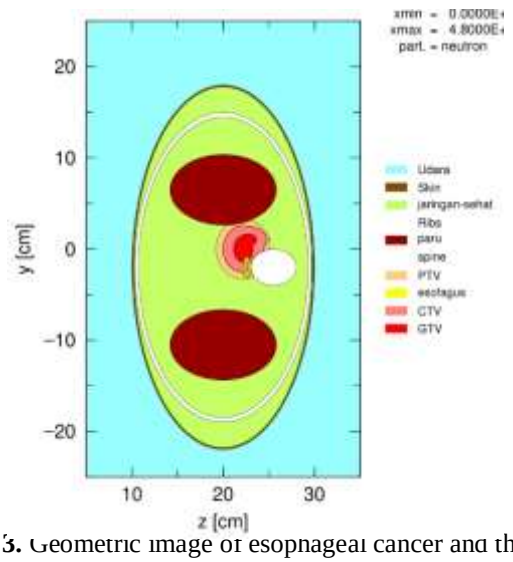

Figure 3. Geometric image of esophageal cancer and the surrounding tissue

3.2 Neutron Source

This research used the HM-30 1 mA cyclotron accelerator from Sumitomo Heavy Industries, which produces a 30 MeV proton beam [36]. In this study, results from replicating the optimization carried out by I Made Ardhana [37] are presented. A BSA collimator generates a suitable neutron flux for the BNCT.

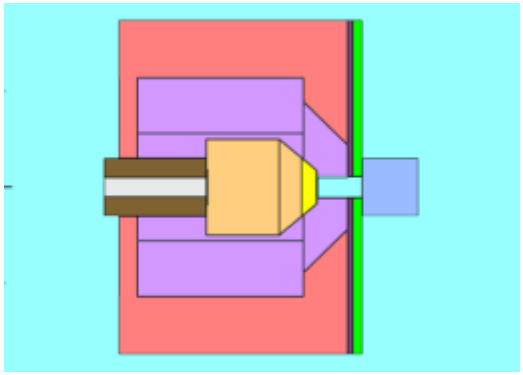

Figure 4. Beam Shaping Assembly Design for BNCT

Table 2. IAEA recommendations for BSA output.

Parameter	IAEA Recommendations	Result
Epithermal Neutron Flux (n/cm^{2}s)	>1.0 × 10^9	1.3 × 10^9
Fast Neutron Dose Rate/Epithermal Neutron Flux (Gy cm^2/n)	<2.0 × 10^{-13}	6.3 × 10^{-14}
Gamma Dose Rate/Epithermal Neutron Flux (Gy cm^2/s)	<2.0 × 10^{-13}	8.3 × 10^{-14}
The ratio of Thermal and Epithermal Neutron Flux (ϕth/ϕepi)	<0.05	0.025
The Ratio of Neutron Current and Neutron Flux (J/ϕepi)	>0.7	0.78

3.3 Monte Carlo Simulation Setup

The simulations in this study were performed using the Particle and Heavy Ion Transport Code System (PHITS) version 3.35. A total of 1.0 × 10^8 particle histories were simulated to ensure adequate statistical reliability of the calculated dose distributions. The associated statistical uncertainty of the tally results ranged from 4% to 50%, depending on the organ region and irradiation geometry. This uncertainty may arise because the measured organ is located quite far from the neutron source, so that only a few particles reach that organ. Meanwhile, in critical target areas, the uncertainty level is usually kept below 5% to ensure the reliability of the reported results.

3.4 Boron Distribution and Carrier Agents

Simulations for esophageal cancer using concentrations of 110 µg/g, 125 µg/g, and 140 µg/g exceeded the minimum threshold recommended for delivering an effective therapeutic dose while protecting healthy tissue. In this study, a boron concentration ratio of 10:5:1 for GTV:CTV: healthy tissue was assumed to reflect the pharmacokinetics of BPA, with CTV receiving 50% and PTV/healthy tissue 10% of the GTV concentration [33]. This is consistent with the pharmacokinetic behavior of BPA, which generally accumulates more in tumor tissue than in normal tissue, thanks to amino acid transport mechanisms [38]. This distribution ensures the selectivity of BNCT, as the neutron–B^{10} reaction occurs preferentially in tumor tissue. In contrast, BSH is distributed more evenly but with lower tumor selectivity. Therefore, the results presented are more representative of BPA-based BNCT, and dose distribution may differ when using BSH.

4. RESULTS AND DISCUSSION

4.1 Radiation Geometry

There are two comparisons between neutron radiation in the AP (Anterior-Posterior) and PA (Posterior-Anterior) directions to determine the most effective radiation direction for esophageal cancer treatment. The AP radiation direction

originates from the front to the back, while the PA direction originates from the back to the front of the patient's body. Both directions target the cancer-affected area directly from the front and back of the patient's body. Figure 5 shows the direction of the BSA collimator design with the ORNL phantom from the AP and PA radiation directions, demonstrating the differences in radiation position and how different directions can affect the distribution of the irradiation beam.

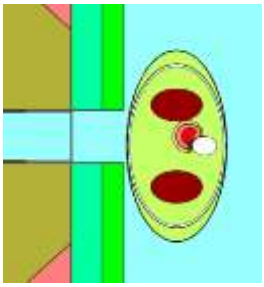

Figure 5. Visualization of Anterior-Posterior (AP) radiation in the axial section.

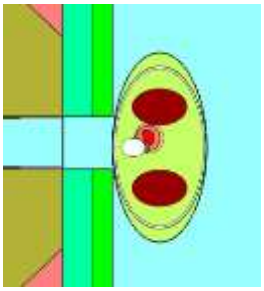

Figure 6. Visualization of Posterior- Anterior (PA) radiation in the axial section.

Based on the geometric data obtained from the PHITS simulation output, there is a significant difference in the length of the irradiation path between the AP and PA directions. In the AP configuration, the distance from the neutron source to the gross tumor volume (GTV) is approximately 11 cm, whereas in the PA direction, this distance is reduced to 6.5 cm. Therefore, irradiation from the PA direction is more effective due to the shorter distance, allowing a higher neutron flux to reach the target tissue. Additionally, the PA beam directly penetrates the tumor, minimizing exposure to surrounding healthy organs (OARs) and resulting in significantly lower doses to these critical structures compared to AP irradiation.

4.2 Neutron Flux

Neutrons are typically categorized into three energy ranges: thermal, epithermal, and fast neutrons. Thermal neutrons possess energies below 0.05 eV, epithermal neutrons range from 0.05 eV to 10 keV, and fast neutrons have energies exceeding 10 keV [14]. During the moderation process, neutrons are redistributed across these energy levels. As epithermal neutrons enter the body, their flux diminishes due to their conversion into thermal neutrons through collisions with atomic nuclei in the tissue, a process known as thermalization. The deeper the epithermal neutrons penetrate the phantom, the more rapidly this thermalization occurs, leading to a progressive reduction in neutron flux [39].

4.3 Total Dose Rate

The results of this study indicate that the boron dose rate is the dominant contributor compared to other components. In both AP and PA irradiation directions, the boron dose rate deposited in the tumor region (GTV) is significantly higher. This contributes substantially to the overall dose rate within the cancerous tissue. As shown in Figure 6, the dose rate at a concentration of 140 µg/g at the anterior direction in the surrounding organs at risk (OARs) remains low, indicating that most BNCT interactions are concentrated within the GTV.

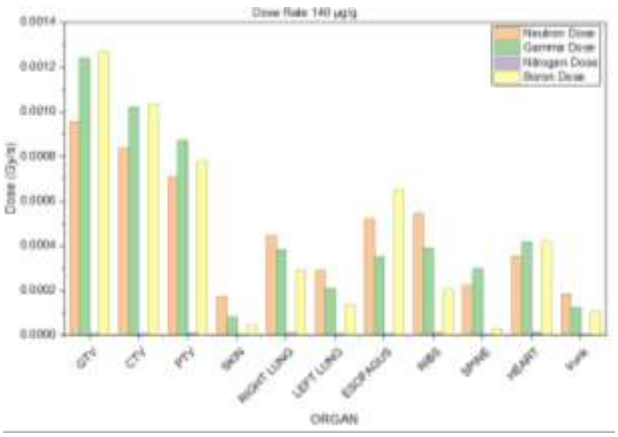

Figure 7. Dose rate neutron, gamma, nitrogen, and boron at 140 µg/g concentration.

The total dose rate is obtained by adding the boron, neutron, gamma, and nitrogen dose rates. The total dose rate is used to evaluate the effectiveness of therapy and the level of exposure to healthy tissue surrounding the tumor. Figures 7 and 8 show the total dose rate absorbed by each organ, in Gy/s.

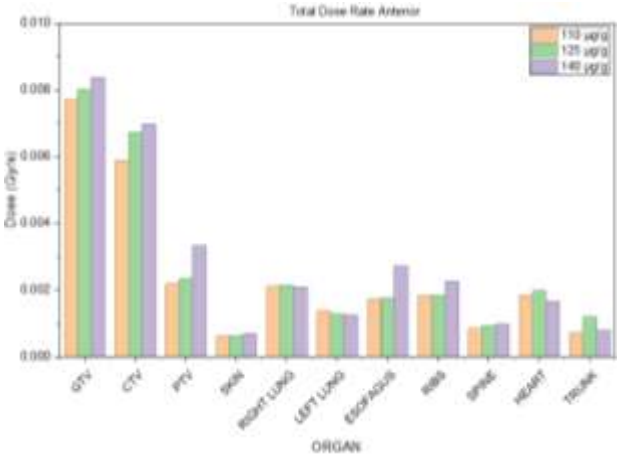

Figure 8. Total dose rate for AP direction

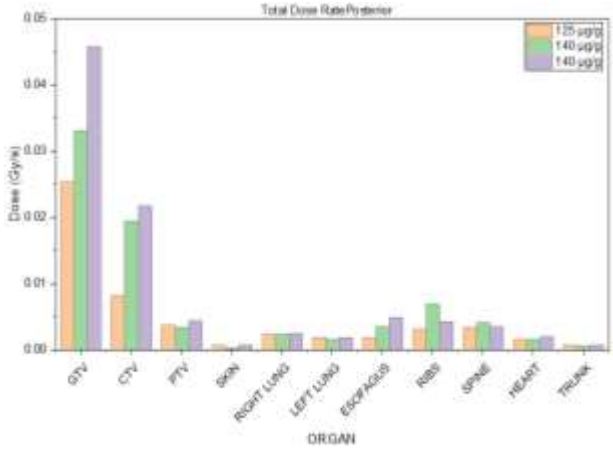

Figure 9. Total dose rate for PA direction

4.4 Irradiation Time

The total dose rate determines the irradiation time required to effectively destroy cancer cells. Figure 6 illustrates the relationship between B-10 concentration and irradiation time. As the amount of boron administered increases, the required irradiation time decreases accordingly.

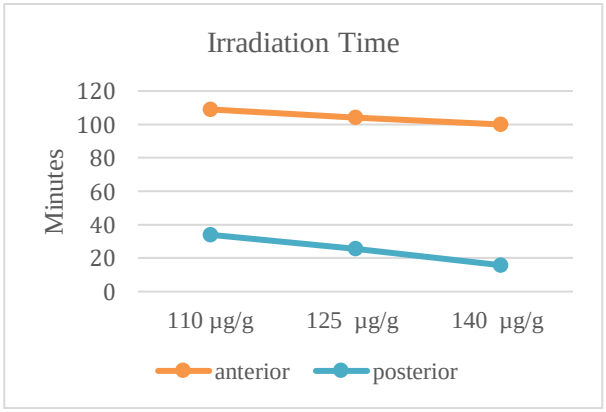

Figure 10. Irradiation time for two directions at three different boron concentrations

Figure 9 shows a decrease in irradiation time with increasing boron concentration from 110 to 140 µg/g, both in the anterior and posterior directions. The irradiation time in the posterior direction was 34 minutes 9 seconds, 25 minutes 45 seconds, and 15 minutes 47 seconds, while in the anterior direction it was 1 hour 49 minutes, 1 hour 44 minutes, and 1 hour 40 minutes 12 seconds. This indicates that irradiation from the posterior direction is more efficient in delivering the therapeutic dose.

4.5 Equivalent Dose

The equivalent dose in BNCT represents the biologically weighted radiation dose, combining contributions from boron reactions, gamma rays, neutrons, and proton recoils. Each component is adjusted using its respective relative biological effectiveness (RBE). In this study, equivalent dose values were obtained from PHITS simulations using the t-track tally and applied multipliers. This allows for evaluating dose distributions to the tumor and surrounding organs at risk, supporting treatment effectiveness and safety analysis. The graph below illustrates the distribution of equivalent dose for both AP and PA irradiation directions at dose levels of 110 µg/g, 125 µg/g, and 140 µg/g.

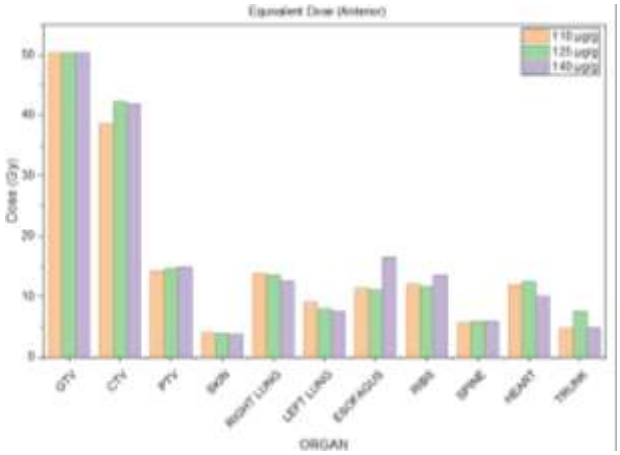

Figure 11. Equivalent dose for AP direction

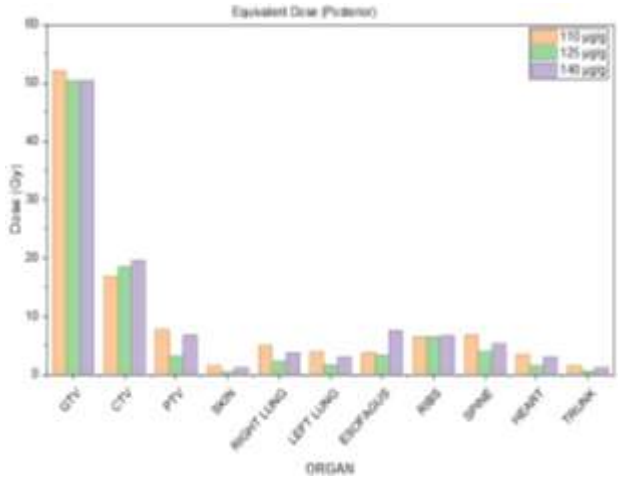

Figure 12. Equivalent dose for PA direction

The equivalent dose is used to describe the biological effects of radiation received by tissue. Equivalent dose is the amount of energy per unit mass absorbed from radiation, corrected by the relative biological effectiveness (RBE) factor. Each organ has a different tolerance limit to avoid damage to that organ. In the esophagus, the acceptable tolerance dose is 15.4 Gy [40]. In the lungs, the acceptable tolerance dose is less than 7.5 Gy; if this dose is exceeded, the lungs may develop pneumonia [40]. For the heart, the tolerance dose limit is 2 Gy; if it exceeds this, it may cause coronary artery disease, pericardial disease, ischemic heart disease, valve disease, and arrhythmia [41]. For the skin, the maximum acceptable dose is 2 Gy. If this dose is exceeded, it can cause acute radiation injury, including erythema, erosion, temporary hair loss, vesicles, pain, and itching, which can last up to 9 weeks [42]. For the ribs and spine, the acceptable dose limit is 14 Gy. Exceeding this dose can cause bone toxicity [40].

The dose absorbed by an organ can be calculated by multiplying the total dose rate by the irradiation time. Of the two irradiation directions tested, a boron concentration of 140 μg/g resulted in the fastest irradiation time, namely 15 minutes for the AP direction and 1 hour and 40 minutes for the PA direction. Table 5 presents the dose received by cancerous and healthy tissues and compares it with the dose tolerance limits for each organ.

Table 3. Equivalent dose of OARs, irradiation direction, and irradiation time

OAR	Irradiation Direction	PA	AP
	Irradiation Time (Min)	100.2	15.78
	Tolerance Dose (Gy)	Equivalent Dose (Gy)	
Esophagus	15.4	3.35	16.5
Left Lung	7.5	1.57	7.52
Right Lung	5	2.26	12.6
Heart	2	1.53	10
Skin	2	0.35	3.76
Spine	14	3.89	5.88
Ribs	14	6.61	13.6

This table compares the radiation doses absorbed by several OARs during AP and PA irradiation techniques, with irradiation times of 48.27 minutes for AP and 9.54 minutes for PA. The data presented includes the tolerance dose and the actual dose absorbed by each organ during irradiation. Overall, the PA technique provides a shorter irradiation time and results in lower doses to critical organs compared to the AP technique. In the right and left lungs, the AP technique produces doses of 12.6 Gy and 7.52 Gy, exceeding the 5 Gy tolerance limit, while the PA technique only produces 2.26 Gy and 1.57 Gy, which are still within safe limits. The dose to the skin also exceeds the 2 Gy tolerance limit when using the AP technique, at 3.76 Gy, while the PA technique only produces 0.35 Gy. For the heart, the AP technique delivers a dose of 10 Gy, exceeding the 2 Gy tolerance limit, while the PA technique remains safe with a dose of 1.53 Gy. For the ribs, both techniques remain within safe limits, at 13.6 Gy (AP) and 6.61 Gy (PA) of the 14 Gy limit. Similarly, the dose to the spine remains below the 14 Gy tolerance limit for both techniques, at 5.88 Gy for AP and 3.89 Gy for PA. Based on this data, the PA technique is safer and recommended as it maintains the absorbed dose to critical organs within the recommended tolerance limits.

A limitation of this study is that dose–volume histograms (DVHs) were not produced because the PHITS simulation used region-based tally instead of voxel-based tally. As a result, only mean organ doses were analyzed, and intra-organ dose heterogeneity could not be evaluated.

5. CONCLUSION

The results of PHITS-based simulations indicate that the posterior–anterior (PA) beam orientation with a boron concentration of 140 μg/g provides more efficient dose delivery to tumor tissue compared to the anterior–posterior (AP) orientation. The PA technique achieved shorter and more consistent irradiation times while maintaining doses to surrounding organs at risk (OARs) within tolerance limits. These findings suggest that the PA configuration may enhance therapeutic efficiency and improve the balance between tumor control and normal tissue protection in BNCT for esophageal cancer.

While these outcomes are promising, it is important to emphasize that they are based solely on computational modeling. The actual clinical feasibility of PA irradiation with elevated boron concentration requires further validation through experimental studies and

clinical trials. Additional investigations are therefore necessary before this approach can be recommended for clinical adoption.

ACKNOWLEDGMENT

We want to express our gratitude to various parties who have contributed to the implementation of this research and the compilation of this journal, including:

1. JAEA, which provided the facilities and infrastructure to support radiotherapy simulations using the PHITS software.
2. The National Research and Innovation Agency (BRIN), organized the MBKM internship program as a platform for this research activity.
3. Maulana Malik Ibrahim State Islamic University of Malang, for the knowledge and academic support provided.

REFERENCES

1. Sung H., *et al.*, "Global Cancer Statistics 2020: GLOBOCAN Estimates of Incidence and Mortality Worldwide for 36 Cancers in 185 Countries," *CA. Cancer J. Clin.*, vol. 71, no. 3, pp. 209–249, 2021, doi: 10.3322/caac.21660.
2. Teng Y., *et al.*, "Esophageal Cancer Global Burden Profiles, Trends, and Contributors," *Cancer Biol. Med.*, vol. 21, no. 8, 2024, doi: 10.20892/j.issn.2095-3941.2024.0145.
3. Park D., Jeon W., J., Yang C., and Castillo D., R., "Advancing Esophageal Cancer Treatment: Immunotherapy in Neoadjuvant and Adjuvant Settings," *Cancers (Basel)*, vol. 16, no. 2, pp. 1–13, 2024, doi: 10.3390/cancers16020318.
4. Kitagawa Y., *et al.*, "Esophageal Cancer Practice Guidelines 2022 Edited by the Japan Esophageal Society: Part 1," *Esophagus*, vol. 20, no. 3, pp. 343–372, 2023, doi: 10.1007/s10388-023-00993-2.
5. Disiena M., Perelman A., Birk J., and Rezaizadeh H., "Esophageal Cancer: An Updated Review," *South. Med. J.*, vol. 114, no. 3, pp. 161–168, 2021, doi: 10.14423/SMJ.0000000000001226.
6. Gamal G., H., "Does PET/CT Give Incremental Staging Information in Cancer Oesophagus Compared to CECT?," *Egypt. J. Radiol. Nucl. Med.*, vol. 50, no. 1, 2019, doi: 10.1186/s43055-019-0114-8.
7. Talasila P., *et al.*, "Imaging in Esophageal Cancer: A Comprehensive Review," *Indian J. Radiol. Imaging*, 2024, doi: 10.1055/s-0044-1786871.
8. Wang H., Xu Y., Zuo F., Liu J., and Yang J., "Immune-based Combination Therapy for Esophageal Cancer," *Front. Immunol.*, vol. 13, no. December, pp. 1–15, 2022, doi: 10.3389/fimmu.2022.1020290.
9. Suzuki S., *et al.*, "Comparison of Lifetime Attributable Risk of Post-irradiation Secondary Cancer of Boron Neutron Capture Therapy, Proton Beam Therapy, and X-ray Therapy for Pediatric and Adolescent and Young Adult Patients," *Clin. Transl. Radiat. Oncol.*, vol. 51, no. October 2024, p. 100921, 2025, doi: 10.1016/j.ctro.2025.100921.
10. Matsumoto Y., Fukumitsu N., Ishikawa H., Nakai K., and Sakurai H., "A Critical Review of Radiation Therapy: From Particle Beam Therapy (Proton, Carbon, and (BNCT) to Beyond," *J. Pers. Med.*, vol. 11, no. 8, 2021, doi: 10.3390/jpm11080825.
11. Conte V., Bianchi A., and Selva A., "Boron Neutron Capture Therapy: Microdosimetry at Different Boron Concentrations," *Appl. Sci.*, vol. 14, no. 1, 2024, doi: 10.3390/app14010216.
12. Yuan T. Z., Xie S. Q., and Qian C., N., "Boron Neutron Capture Therapy of Cancer: Critical Issues and Future Prospects," *Thorac. Cancer*, vol. 10, no. 12, pp. 2195–2199, 2019, doi: 10.1111/1759-7714.13232.
13. Monti Hughes A. and Hu N., "Optimizing Boron Neutron Capture Therapy (BNCT) to Treat Cancer: An Updated Review on the Latest Developments on Boron Compounds and Strategies," *Cancers (Basel).*, vol. 15, no. 16, pp. 1–30, 2023, doi: 10.3390/cancers15164091.
14. Shuai H., Dian E., Mezei F., Sipos P., and Czifrus S., "An Accelerator-based Neutron Source Design with a Thermal Neutron Port and an Epithermal Neutron Port for Boron Neutron Capture Therapy," *Appl. Radiat. Isot.*, vol. 217, no. August 2024, 2025, doi: 10.1016/j.apradiso.2024.111647.
15. Shlinamd Anderson P., More Xin Wang S., Peter Van Rossum S., N., Yan Chu M., D., Tucker Netherton, Radhe Mohan, Steven H., Lin, M., D., "Severe Lymphopenia During Chemoradiation Therapy for Esophageal Cancer: Comprehensive Analysis of Randomized Phase 2B Trial of Proton Beam Therapy Versus Intensity Modulated Radiation Therapy," *Int. J. Radiat. Oncol. Biol. Phys.*, vol. 118, no. 2, pp. 368–377, 2024.

16. Kakino R. *et al.*, "Out-of-field Dosimetry using a Validated PHITS Model and Computational Phantom in Clinical BNCT," *Med. Phys.*, vol. 51, no. 2, pp. 1351–1363, 2024, doi: 10.1002/mp.16916.
17. Nishitani T., *et al.*, "Neutronics Analyses of the Radiation Field at the Accelerator-Based Neutron Source of Nagoya University for the BNCT Study," *J. Nucl. Eng.*, vol. 3, no. 3, pp. 222–232, 2022, doi: 10.3390/jne3030012.
18. Green S., *et al.*, "Accelerator Neutron Sources for BNCT: Current Status and Some Pointers for Future Development," *Appl. Radiat. Isot.*, vol. 217, no. October 2024, p. 111656, 2025, doi: 10.1016/j.apradiso.2025.111656.
19. Li G., Jiang W., Zhang L., Chen W., and Li Q., "Design of Beam Shaping Assemblies for Accelerator-Based BNCT With Multi-Terminals," *Front. Public Heal*, vol. 9, no. March, pp. 1–10, 2021, doi: 10.3389/fpubh.2021.642561.
20. Hattori Y., *et al.*, "Proposal of Recommended Experimental Protocols for in Vitro and in Vivo Evaluation Methods of Boron Agents for Neutron Capture Therapy," *J. Radiat. Res.*, vol. 64, no. 6, pp. 859–869, 2023, doi: 10.1093/jrr/rrad064.
21. Zhang Z. *et al.*, "A Review of Planned, Ongoing Clinical Studies and Recent Development of BNCT in Mainland of China," *Cancers (Basel)*, vol. 15, no. 16, 2023, doi: 10.3390/cancers15164060.
22. Fukuda H., "Response of Normal Tissues to Boron Neutron Capture Therapy (BNCT) with 10 B-borocaptate Sodium (BSH) and 10 B-paraboronophenylalanine (BPA)," *Cells*, vol. 10, no. 11, 2021, doi: 10.3390/cells10112883.
23. Fukuda H., "Boron Neutron Capture Therapy (BNCT) for Cutaneous Malignant Melanoma using 10 b-p-boronophenylalanine (BPA) with Special Reference to the Radiobiological Basis and Clinical Results," *Cells*, vol. 10, no. 11, 2021, doi: 10.3390/cells10112881.
24. Dymova M., A., Taskaev S., Y., Richte V., A., and Kuligina E., V., "Boron Neutron Capture Therapy: Current Status and Future Perspectives," *Cancer Commun.*, vol. 40, no. 9, pp. 406–421, 2020, doi: 10.1002/cac2.12089.
25. Wang Z., *et al.*, "Recent Research Progress of BNCT Treatment Planning System," *Nucl. Eng. Technol.*, vol. 57, no. 3, p. 103264, 2024, doi: 10.1016/j.net.2024.10.026.
26. Yusuke Matsuya T., K., Yuji Yoshii, Tamon Kusumoto, Ken Akamatsu, Yuho Hirata, Tatsuhiko Sato, "A Step-by-step Simulation Code for Estimating Yields of Water Radiolysis Species based on Electron Track-structure Mode in the PHITS Code," *Phys. Med. Biol.*, vol. 69, no. 3, 2024.
27. Sato T., *et al.*, "Recent Improvements of the Particle and Heavy Ion Transport Code System–PHITS Version 3.33," *J. Nucl. Sci. Technol.*, vol. 61, no. 1, pp. 127–135, 2024, doi: 10.1080/00223131.2023.2275736.
28. CarterL., M., *et al.*, "PARaDIM: A PHITS-Based Monte Carlo Tool for Internal Dosimetry with Tetrahedral Mesh Computational Phantoms," *J. Nucl. Med.*, vol. 60, no. 12, pp. 1802–1811, 2019, doi: 10.2967/jnumed.119.229013.
29. Ogawa T., Hirata Y., Matsuya T., Kai T., Sato T., and Iwamoto Y., "Overview of PHITS Ver . 3 . 34 with Particular Focus on Track-structure Calculation," vol. 13, 2024.
30. Kumada H., and Takada K., "Treatment Planning System and Patient Positioning for Boron Neutron Capture Therapy," *Ther. Radiol. Oncol.*, vol. 2, pp. 50–50, 2018, doi: 10.21037/tro.2018.10.12.
31. Hu N., *et al.*, "Evaluation of a Treatment Planning System Developed for Clinical Boron Neutron Capture Therapy and Validation Against an Independent Monte Carlo dose calculation system," *Radiat. Oncol.*, vol. 16, no. 1, pp. 1–13, 2021, doi: 10.1186/s13014-021-01968-2.
32. Bilalodin B., Wihantoro, Haryadi A., and Abdullatif F., "Dosimetry Analysis of Boron Neutron Capture Therapy (BNCT) on Thyroid Cancer using PHITs Code with Neutron from 30 MeV Cyclotron," *J. Teknol.*, vol. 85, no. 5, pp. 21–26, 2023, doi: 10.11113/jurnalteknologi.v85.19454.
33. Harish A., F., Warsono, and Sardjono Y., "Dose Analysis of Boron Neutron Capture Therapy (BNCT) Treatment for Lung Cancer Based on Particle and Heavy Ion Transport Code System (PHITS)," *ASEAN J. Sci. Technol. Dev.*, vol. 35, no. 3, pp. 187–194, 2020, doi: 10.29037/ajstd.545.
34. Han D., *et al.*, "Neoadjuvant Radiation Target Volume Definition in Esophageal Squamous Cell Cancer: a Multicenter Recommendations from Chinese Experts," *BMC Cancer*, vol. 24, no. 1, 2024, doi: 10.1186/s12885-024-12825-2.

35. Lee S., L., Bassetti M., Meijer G., J., and Mook S. "Review of MR-Guided Radiotherapy for Esophageal Cancer," *Front. Oncol.*, vol. 11, no. March, pp. 1–8, 2021, doi: 10.3389/fonc.2021.628009.
36. Tanaka H., *et al.*, "Characteristic Evaluation of the Thermal Neutron Irradiation Field using a 30 MeV Cyclotron Accelerator for Basic Research on Neutron Capture Therapy," *Nucl. Instruments Methods Phys. Res. Sect. A Accel. Spectrometers, Detect. Assoc. Equip.*, vol. 983, 2020.
37. Ardana I., M., and Sardjono Y., "Optimization of a Neutron Beam Shaping Assembly Design for Bnct and Its Dosimetry Simulation Based on Mcnpx," *J. Teknol. Reakt. Nukl. Tri Dasa Mega*, vol. 19, no. 3, p. 121, 2017, doi: 10.17146/tdm.2017.19.3.3582.
38. Hattori Y., *et al.*, "Proposal of Recommended Experimental Protocols for In Vitro and In Vivo Evaluation Methods of Boron Agents for Neutron Capture Therapy," Nov. 01, 2023, *Oxford University Press*. doi: 10.1093/jrr/rrad064.
39. Li G., Jiang W., Zhang L., Chen W., and Li Q., "Design of Beam Shaping Assemblies for Accelerator-Based BNCT With Multi-Terminals," *Front. Public Heal.*, vol. 9, pp. 1–10, 2021, doi: 10.3389/fpubh.2021.642561.
40. Yu H., *et al.*, "Impacts of Mfield Irradiation and Boron Concentration on the Treatment of Boron Neutron Capture Therapy for Non-small Cell Lung Cancer," *Int. J. Radiat. Res.*, vol. 15, no. 1, pp. 1–13, 2017, doi: 10.18869/acadpub.ijrr.15.1.1.
41. Holt F., *et al.*, "Estimated Doses to the Heart, Lungs and Oesophagus and Risks From Typical UK Radiotherapy for Early Breast Cancer During 2015–2023," *Clin. Oncol.*, vol. 36, no. 9, pp. e322–e332, 2024, doi: 10.1016/j.clon.2024.05.002.
42. Jaschke W., Schmuth M., Trianni A., and Bartal G., "Radiation-Induced Skin Injuries to Patients: What the Interventional Radiologist Needs to Know," *Cardiovasc. Intervent. Radiol.*, vol. 40, no. 8, pp. 1131–1140, 2017, doi: 10.1007/s00270-017-1674-5.

APPENDIX